

Instability of Population III Black Hole Accretion Disks

Ken OHSUGA,^{1,2} Hajime SUSA,^{2,3} and Yosuke UCHIYAMA²

¹*Institute of Physical and Chemical Research (RIKEN), 2-1, Hirosawa, Wako, Saitama 351-0198*

²*Department of Physics, Rikkyo University, Toshima-ku, Tokyo 171-8501*

³*Department of Physics, Konan University 8-9-1 Okamoto, Kobe 658-8501*

(Received 2007 April 9; accepted 2007 July 27)

Abstract

We investigate the stability of black hole accretion disks in a primordial environment (POP III disks for short), by solving the vertical structure of optically thick disks, including convective energy transport, and by employing a one-zone model for optically thin isothermal disks. Because of the absence of metals in POP III disks, we find significant differences in stability associated with ionization between POP III disks and the disks of solar metallicity. An unstable branch in S-shaped equilibrium curves on the $\dot{M} - \Sigma$ (mass accretion rate - surface density) plane extends to a larger surface density compared with the case of disks of solar metallicity. The resulting equilibrium loci indicate that quasi-periodic oscillations in luminosity can also be driven in POP III disks, and their maximal luminosity is typically by an order of magnitude larger than that of the disks of solar metallicity. Such a strong outburst of POP III disks can be observed by future huge telescopes, in case that the mass is supplied onto the disks at the Bondi accretion rates in typical virialized small dark halos.

Key words: accretion, accretion disks — black hole physics — instabilities — cosmology: early universe

1. Introduction

According to recent advances in the formation theory of population III (POP III) stars, it has been understood that they could be very massive ($10^2 - 10^3 M_\odot$) (Omukai & Nishi 1998; Abel et al. 2000; Bromm et al. 2002).

Those stars end up as black holes as massive as $10 - 10^3 M_\odot$ (here after POP III BHs), in the case that the mass of the progenitor stars is within the range $40 M_\odot \lesssim M_* \lesssim 140 M_\odot$ or $M_* \gtrsim 260 M_\odot$ (Heger & Woosly 2002). The accretion disks formed around such black holes can emit a significant amount of soft X-rays, which can contribute to reionization of the universe (Ricotti & Ostriker 2004). Moreover, such black holes could be candidates for the progenitors of ultra-luminous X-ray sources (Mii & Totani 2005) or the building blocks of super-massive black holes (Rees 1984).

The accretion disks surrounding POP III BHs are formed from the accreting gas around the progenitor stars. In the case that the mass of a POP III star is within the range $40 M_\odot \lesssim M_* \lesssim 140 M_\odot$ or $M_* \gtrsim 260 M_\odot$, the star forms a black hole directly without a SN (Heger & Woosly 2002). In this case, the accreting gas is expected to contain a small amount of heavy elements. In addition, recent numerical simulations on low-mass galaxy formation, taking into account the effects of SNe feedback, suggest that the metallicity of the gas remain in such galaxies during their early star-burst phase is as low as $\sim 10^{-4} Z_\odot$ (Wada & Venkatesan 2003). Therefore, the metallicity of the accretion disks surrounding POP III BHs is expected to be very low ($Z \lesssim 10^{-4} Z_\odot$). We hereafter call these accretion disks as POP III disks.

The thermal instability of the standard accretion disk has been investigated in detail (e.g. Shibazaki & Hōshi 1975; Shakura & Sunyaev 1976; Pringle 1976). By assuming solar metallicity (hereafter POP I disks), Mineshige and Osaki (1983) obtained the S-shaped equilibrium loci on the $\dot{M} - \Sigma$ (mass accretion rate v.s. surface density) plane, implying that the unstable disk undergoes limit-cycle oscillation between the upper, hot, ionised branch and the lower, cool neutral branch (see also Hōshi 1979; Meyer & Meyer-Hofmeister 1981; Smak 1982; Kato et al. 1998 for a review). It is so-called dwarf-nova type instability, which successfully explains the observed properties of dwarf nova (Meyer & Meyer-Hofmeister 1984). An X-ray nova is also thought to be caused by such a disk instability, although its central object is expected to be a black hole (Huang & Wheeler 1989; Mineshige & Wheeler 1989). The limit-cycle behavior for active galactic nuclei has been investigated by Lin & Shields (1986) (see also Mineshige & Shields 1990).

Mayer and Duschl (2005) investigated this instability on the POP III disks in which they also obtained the equilibrium loci on the $\dot{M} - \Sigma$ plane. However, their results based upon a one-zone approximation, even if the disk is optically thick, in which the energy transfer due to convection along the direction perpendicular to the equatorial plane of the disk is not included. As a result, the equilibrium loci are not S-shaped, which does not directly lead to the limit-cycle oscillations driven by thermal and secular instabilities. Thus, we need a more sophisticated approach in order to understand the nature of the stability of POP III disks. In this paper, we re-examine stability of POP III disks, by solving the vertical structure of optically thick disks, including the effect of convection. For optically thin

disks, we adopt a one-zone approximation. In addition, we evaluate the amplification of the luminosity of accretion disks surrounding POP III BHs by the limit-cycle oscillation. We also discuss the possibility to detect the POP III disks by calculating their emergent spectra in the burst phase.

This paper is organised as follows: we describe basic equations in section 2. We compare the stability of POP III disks with POP I disks in section 3. In section 4, we discuss the observational possibility of POP III black hole accretion disks, and summarise in the final section.

2. Model and Numerical Method

2.1. Optically Thick Regime

In this subsection, we show the basic equations used to describe the vertical structure of the optically-thick accretion disks. Here, we assume that the disks are in hydrostatic equilibrium along the vertical axis, and local energy balance is attained. The convective energy transport is taken into consideration. The equation of hydrostatic equilibrium is given by

$$\frac{dp}{dz} = -\rho \frac{GMz}{r^3}, \quad (1)$$

where p is the total pressure, ρ is the density, M is the black hole mass, and r and z are the radial and vertical coordinates. The equation of energy transport is

$$\frac{d \ln T}{d \ln z} = \begin{cases} \nabla_{\text{rad}} & (\nabla_{\text{rad}} < \nabla_{\text{ad}}) \\ \nabla_{\text{conv}} & (\nabla_{\text{rad}} > \nabla_{\text{ad}}) \end{cases}, \quad (2)$$

where T is the temperature, and ∇_{ad} is the adiabatic gradient.

The radiative gradient, ∇_{rad} , is written as

$$\nabla_{\text{rad}} = \frac{3r^3 \kappa p F}{4acT^4 GMz}, \quad (3)$$

where κ represents the opacity, F and a denote the energy flux and the radiation constant, respectively. We utilise the latest OPAL opacity table¹ including low temperature opacities (Ferguson et al. 2005). The energy flux is evaluated by integrating the following equation, which represents the local energy balance :

$$\frac{dF}{dz} = -\frac{3}{2} \alpha p \Omega. \quad (4)$$

Here α is the viscosity parameter, whereas $\Omega = (GM/r^3)^{1/2}$ represents the Keplerian angular speed. We employ the expression $\alpha = \min[1.0, 10^2(H/r)^{1.5}]$ (with H being the disk half thickness), which succeeds to reproduce the variation amplitude and the timescale of the X-ray novae (Kato et al. 1998, see also Meyer & Meyer-Hofmeister 1984), whereas the viscosity model is still poorly understood for the primordial composition. We here note that the source of disk viscosity is thought to be of magnetic origin based on the recent magnetohydrodynamic simulations (Hawley et al. 2001; Machida et al. 2001; Balbus 2003, for a review).

The convective gradient, ∇_{conv} , is calculated by the mixing-length formalism for convection (Paczýński 1969), in which we assume mixing length, l , to be

$$l = \min(H, H_p), \quad (5)$$

where H_p is the pressure scale height.

In order to close the set of equations (1)-(5), we need the equation of state for the system in radiative equilibrium,

$$p = \frac{\rho k T}{\mu m_p} + \frac{1}{3} a T^4, \quad (6)$$

where m_p denotes the proton mass, k represents the Boltzmann constant, and μ is the mean molecular weight.

We integrate equations (1), (2), and (4) from the disk surface ($z = H$) toward the equatorial plane ($z = 0$) by the Runge-Kutta method for given parameters, r , Z , and \dot{M} , where Z is the metallicity and \dot{M} is the mass accretion rate. The outer boundary ($z = H$) conditions for temperature, energy flux, pressure are given by

$$T = \left(\frac{3}{8\pi} \frac{GM\dot{M}}{\sigma r^3} \right)^{1/4}, \quad (7)$$

$$F = \sigma T^4, \quad (8)$$

and

$$p = \frac{2}{3\kappa} \Omega^2 H, \quad (9)$$

where σ denotes the Stefan-Boltzmann constant. We iteratively search H so as to meet the condition $F = 0$ at $z = 0$. Then, we obtain the vertical structure of the accretion disks. In this method, the column density and the optical thickness are calculated from $\Sigma = 2 \int_0^H \rho dz$ and $\tau = \int_0^H \rho \kappa dz$, respectively. This method breaks down in the regions of a small mass accretion rate for POP III disks, since then the disks become optically thin (We will discuss this point later). A numerical method for optically thin disks is described in the next subsection.

2.2. Optically Thin Regime

The optically thin disks would be nearly isothermal, in which convection does not contribute to the energy transport and the radiative diffusion approximation breaks down. Here, we adopt a one-zone model for optically thin disks. Since the radiation pressure is negligible in the optically thin medium, the equation of hydrostatic equilibrium is given by

$$\Omega^2 H^2 = \frac{p_{\text{gas}}}{\rho}, \quad (10)$$

where $p_{\text{gas}} = \rho k T / \mu m_p$ is the gas pressure. The viscous heating rate is described as

$$Q_{\text{vis}} = -\frac{3}{2} T_{r\varphi} \Omega, \quad (11)$$

where $T_{r\varphi}$ is the shear stress tensor. Using the alpha-prescription, $T_{r\varphi} = -2\alpha p_{\text{gas}} H$, we rewrite the equation (11) as

¹ <http://www-phys.llnl.gov/Research/OPAL/opal.html>

$$Q_{\text{vis}} = \frac{3}{2} \alpha \frac{p_{\text{gas}}}{\rho} \Omega \Sigma, \quad (12)$$

where $\Sigma = 2\rho H$ is the column density. The viscosity parameter, α , is given by $\alpha = \min[1.0, 10^2(H/r)^{1.5}]$, the same as in the method for the optically thick disks. The radiative cooling rate is written as

$$Q_{\text{rad}} = 2\sigma T^4 \tau, \quad (13)$$

where $\tau = \kappa \Sigma / 2$ is the optical thickness of the disk. Combining the energy balance equation ($Q_{\text{vis}} = Q_{\text{rad}}$) and equation (10), we obtain the physical quantities of the disks.

To calculate the mass-accretion rate, we use the continuity equation ($\dot{M} = \text{const.}$ in r -direction) and the angular-momentum conservation law. By assuming a torque-free boundary condition and angular momentum of the gas to be much smaller at the inner boundary than at the outer region, we have

$$T_{r\phi} = -\frac{1}{2\pi} \sqrt{\frac{GM}{r^3}} \dot{M}. \quad (14)$$

Thus, using equation (11) and (14), the mass-accretion rate is given by

$$\dot{M} = \frac{4\pi}{3} \frac{r^3}{GM} Q_{\text{vis}}. \quad (15)$$

Throughout the present study, we set the black hole mass to be $M = 10^3 M_{\odot}$, unless stated otherwise.

3. Results

In figure 1, we present the sequence of equilibrium curves on the $\dot{M} - \Sigma$ (mass accretion rate - surface density) plane for $r = 10^4 r_{\text{S}}$ with $Z/Z_{\odot} = 0, 10^{-4}$, and 1, where $r_{\text{S}} \equiv 2GM/c^2$ denotes the Schwarzschild radius. Here, the thick and thin solid lines indicate the resulting equilibrium loci for optically thick accretion disks with $\tau \geq 3$, in which the energy is transported via convection as well as radiative diffusion (see §2.1), and the optically thin isothermal disks with $\tau \leq 0.3$ (see §2.2). Our numerical method for optically thick disks gives optically thin branches for POP III disks when $\dot{M} \lesssim 10^{-7} M_{\odot}/\text{yr}$. Although they are unphysical branches, we represent them by the dotted lines.

We find that the optically-thick POP III disks transit to the optically-thin isothermal disks at around $\dot{M} \sim 10^{-7} M_{\odot}/\text{yr}$. In contrast, the POP I disks stay optically thick ($\tau \geq 3$), even if the mass-accretion rate is less than $10^{-7} M_{\odot}/\text{yr}$. We find that all curves have two major turning points at $\dot{M} \sim 10^{-7} M_{\odot}/\text{yr}$ (lower-right turning point) and $10^{-6} M_{\odot}/\text{yr}$ (upper-left turning point), where the gradients of the curves, $\partial \dot{M} / \partial \Sigma$, change their signs. In other words, the S-shaped equilibrium curves appear irrespective of the metallicity. It is known that the middle branch ($\partial \dot{M} / \partial \Sigma < 0$: between the upper-left and lower-right turning points) is thermally and secularly unstable, whereas the disk is stabilised in upper and lower branches, along which $\partial \dot{M} / \partial \Sigma > 0$ being satisfied.

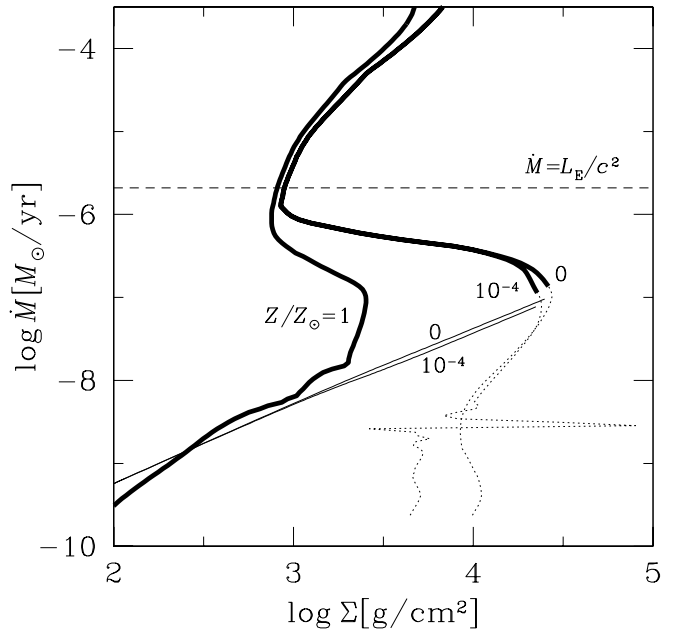


Fig. 1. Sequence of equilibrium curves of the optically-thick accretion disks with $\tau \geq 3$ (the thick solid lines) and the optically-thin isothermal disks with $\tau \leq 0.3$ (the thin solid lines) for $Z/Z_{\odot} = 0, 10^{-4}$, and 1. The dotted lines are equilibrium loci for POP III disks with $\tau < 3$, which is obtained by the method described in §2.1, although this method might break down there. The dashed line indicates the critical mass-accretion rate, L_{E}/c^2 , where L_{E} is the Eddington luminosity. The adopted parameters are $M = 10^3 M_{\odot}$ and $r = 10^4 r_{\text{S}}$.

Figure 1 indicates that if the mass-accretion rate falls within the range $10^{-7} M_{\odot}/\text{yr} \lesssim \dot{M} \lesssim 10^{-6} M_{\odot}/\text{yr}$, the POP III disks exhibit the limit-cycle behaviour, as well as the POP I disks (Mineshige & Osaki 1983), since no stable branch exists. Note that the range of the mass-accretion rate, which induces the limit-cycle behavior, increases as the radius increases. We discuss this point in §4.1. When the disk stays in the lower stable branch, the surface density at $r = 10^4 r_{\text{S}}$ increases with time, because the mass input rate (mass supplied from outside per unit time) is larger than the mass-output rate (mass ejected inward per unit time). As a result, the disk evolves along the lower stable branch toward the lower-right turning point on the $\dot{M} - \Sigma$ plane (quiescent state). After a while, it suddenly jumps to the upper branch at the right end of the stable branch (lower-right turning point). Since the mass-input rate is smaller than the mass-output rate in the upper stable branch, Σ decreases along the upper stable branch toward the upper-left turning point (burst state) until it jumps back to the lower branch. Thus, quasi-periodic oscillation of the mass-accretion rate onto the black hole is caused by such state transitions of the disk, leading to oscillations in luminosity.

Here, we stress that the S-shaped equilibrium curve of the POP III disks, as well as the POP I disks, does not

appear if we employ the one-zone approach for optically thick disks (see figure 4 in Mayer & Duschl 2005). It is crucial to solve the vertical structure of the optically thick disks, including the convective effect, in order to investigate the bursting phenomenon caused by a dwarf-nova type instability.

Although the limit-cycle oscillations could arise both in POP I and POP III disks, the POP III disks exhibit stronger outbursts than do the POP I disks. The surface density at the lower-right turning point is about an order of magnitude larger in the POP III disks than in the POP I disks, whereas the upper stable branch is independent of the metallicity. Consequently, the luminosity of POP III disks is about an order of magnitude larger than that of the POP I disks just after a state transition from the quiescent to burst states. As shown in figure 1, the equilibrium loci for $Z/Z_\odot = 0$ and 10^{-4} almost overlap each other. It implies that the magnitude of the outburst is independent of the metallicity as long as $Z/Z_\odot \lesssim 10^{-4}$ is satisfied. Here, we note that the S-shaped equilibrium curves for $Z/Z_\odot \gtrsim 10^{-3}$ deviate significantly from those for the POP III disks, although we do not plot them in this figure. Whereas the upper branch does not depend upon Z very much, the lower turning point shifts toward the left side as the metallicity increases for $Z/Z_\odot \gtrsim 10^{-3}$.

Since we have $\alpha \sim 1$ and $T \sim 10^5 \text{K}$ in the upper branch, the timescale of the burst phase is evaluated to be

$$t_b \sim 2.1\alpha^{-1} \left(\frac{M}{10^3 M_\odot} \right)^{1/2} \times \left(\frac{r}{10^4 r_S} \right)^{1/2} \left(\frac{T}{10^5 \text{K}} \right)^{-1} \text{ yr.} \quad (16)$$

This timescale is basically the viscous timescale. The timescale for the quiescent phase is given by $\pi r^2 \Sigma / \dot{M}$. It is described as

$$t_q \sim 4.2 \times 10^2 \left(\frac{r}{3 \times 10^{12} \text{cm}} \right)^2 \times \left(\frac{\Sigma}{3 \times 10^4 \text{g cm}^{-2}} \right) \left(\frac{\dot{M}}{10^{-6} M_\odot \text{yr}^{-1}} \right)^{-1} \text{ yr.} \quad (17)$$

The disc evolves along the lower stable branch on this timescale, and it attains the lower-right turning point. The timescales of the burst and quiescent phases are much longer than those of the transition between the burst and quiescent states. Hence, about $\epsilon = t_b/t_q \sim 0.5\%$ of the unstable POP III disks would stay in the burst state, which are observed as very luminous objects. Here, we remark that global calculations of the disks are need for investigating the time evolution of the disks in detail.

In figure 1, we find that the mass-accretion rate exceeds the critical rate in the burst phase. In this phase, H/r is comparable to, or slightly larger than, unity, although the disk is assumed to be geometrically thin in our method. The radiation pressure-dominated region would appear at the inner region of the disk, in which the disk is unstable if the viscosity is proportional to the total pressure. Such

coupling of two instabilities has been suggested by Lin and Shields (1986). By supercritical accretion, the radiatively driven outflows would form in the vicinity of the black hole, and the photon would be trapped in the flow within the trapping radius, $r_{\text{trap}} \sim (\dot{M} c^2 / L_E) r_S$ (Ohsuga et al. 2002). We need a global multi-dimensional approach to investigate the disk structure in detail (e.g., Ohsuga et al. 2005; Ohsuga 2006; 2007). However, it is beyond the scope of the present study.

The irradiation flux is not taken into consideration in the present study. Tuchman et al. (1990) has reported that convective disks are stabilized by strong irradiation with $T > 10^4 \text{K}$. However, it is not easy to get the irradiation flux, since it is very sensitive to the geometry and the radiative processes. In the quiescent phase, the disk is very geometrically thin, so that the irradiation flux would be reduced. In the burst phase, the thick disk forms via the supercritical accretion. Then, the radiative flux is collimated in the polar direction, suppressing the irradiation effect (Ohsuga et al. 2005). The self-occultation by the thick disk would also reduce the irradiation flux (Watarai et al. 2005). For this issue, we should study the global structure of the disks, fully accounting for radiative transfer in the multi-dimensional space.

In figure 2, we represent the resulting optical thickness of the accretion disks, which are obtained by the method described in §2.1, as functions of the mass-accretion rate. As shown in this figure, the disks are very optically thick in the upper stable branch (burst state), $\dot{M} \gtrsim 10^{-6} M_\odot \text{yr}^{-1}$. Hence, the spectral energy distributions (SEDs) are thought to consist of the superposition of the blackbody spectra with various temperatures at the disk surface. We show them in §4.

In contrast, as mentioned above, the POP III disks are optically thin in the regime of $\dot{M} \lesssim 10^{-7} M_\odot \text{yr}^{-1}$. Such results are unphysical, since our method described in §2.1 is available only if the disks are optically thick. The POP I disks are optically thick, even in the case of $\dot{M} \lesssim 10^{-7} M_\odot \text{yr}^{-1}$. Cannizzo and Wheeler (1984) reported that POP I disks become optically thin for a small mass-accretion rate in the case of $\alpha \gtrsim 0.1$, and disks with smaller α stay optically thick down to a far lower mass-accretion rate. Since α is around 0.03 in the present work, our results are consistent with their study.

In the middle unstable branch, where $10^{-7} M_\odot \text{yr}^{-1} \lesssim \dot{M} \lesssim 10^{-6} M_\odot \text{yr}^{-1}$ is satisfied, the optical thickness increases very rapidly with an increase of the mass-accretion rate. Hence, even in the case of POP III disks, the optical thickness is very large in the upper stable and middle unstable branches.

It is found that the spiky structure appears around $\dot{M} = 10^{-8.5} M_\odot \text{yr}^{-1}$ for $Z/Z_\odot = 10^{-4}$. The feature is due to the line opacity for heavy elements. Such opacity is very sensitive to the temperature as well as the density. Since the matter does not contain the heavy elements for $Z = 0$, and since dust cooling is dominant over line cooling for $Z = Z_\odot$, the spiky structure appears only in the case of intermediate metallicity.

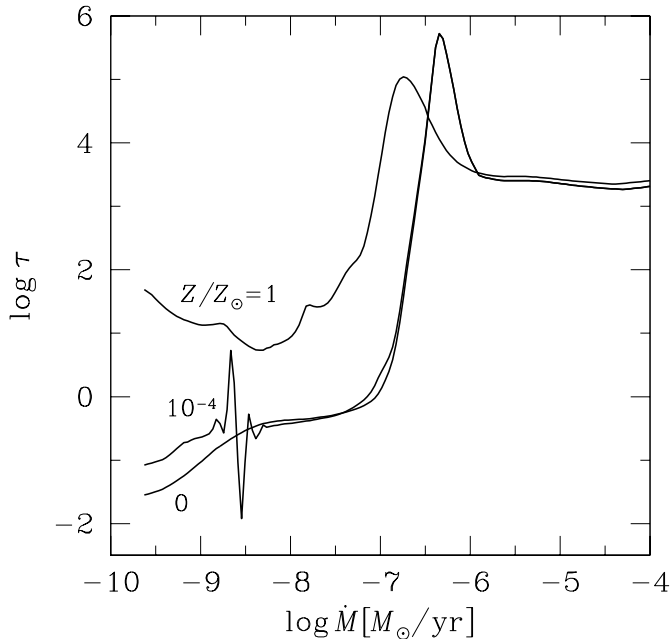


Fig. 2. Optical thickness of disks for $Z/Z_{\odot} = 0, 10^{-4}$, and 1 as functions of the mass-accretion rate, where we use the method described in §2.1. Our method, in which we assume the disk to be optically thick, breaks down for POP III disks with $\dot{M} \lesssim 10^{-7} M_{\odot} \text{yr}^{-1}$.

4. Discussion

4.1. SED of POP III disks

We have so far discussed S-shaped equilibrium curves, which predict the potential possibility of limit-cycle behaviour in POP III disks via thermal and secular instabilities. We are now ready to discuss whether the limit-cycle oscillations are activated in realistic environments surrounding POP III disks, or not.

If we consider black holes in halos with $M_{\text{halo}} \sim 10^8 M_{\odot}$ at $z \sim 20$, the virial temperatures of these halos are typically $T \sim 10^4 \text{K}$, from which the gas is not evacuated by radiative feedback of the progenitor star (Kitayama et al. 2004).

The density of the gas surrounding the black holes would be comparable to, or larger than that of the virialized halos (Kitayama et al. 2004). Thus, in the first place, we assess the mass-accretion rate from the host halo to the accretion disk by the Bondi accretion rate with the given virialized density/temperature of the halo.

In figure 3, by using the method described in §2.1, we plot the resulting sequence of equilibrium curves of disks for $r = 10^3 r_S$, $3 \times 10^3 r_S$, and $10^4 r_S$ with $Z/Z_{\odot} = 10^{-4}$ (the solid lines). Here, the disks are optically thick, $\tau \geq 3$, on the thick solid lines. In contrast, our method described in §2.1 gives the optically thin solutions below the lower turning points (see the thin solid lines), although this method is available only for optically thick disks. We also show the

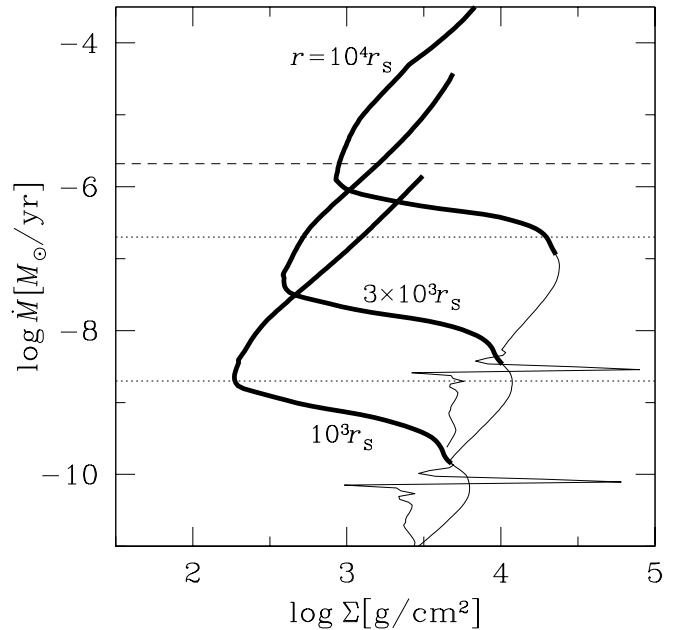


Fig. 3. Sequence of equilibrium curves of the accretion disks for $r = 10^3 r_S$ (the lower solid lines), $r = 3 \times 10^3 r_S$ (the middle solid lines), and $10^4 r_S$ (the upper solid lines) in the case of $Z/Z_{\odot} = 10^{-4}$. Here, we use the method described in §2.1, although the disks are assumed to be optically thick in this method. The thick and thin solid lines are equilibrium loci for the disks with $\tau \geq 3$ and $\tau < 3$, respectively. Two dotted lines indicate the Bondi accretion rates for $\rho(\infty) = 10^{-22} \text{g cm}^{-3}$ (upper) and $10^{-24} \text{g cm}^{-3}$ (lower). The critical accretion rate is represented by the dashed line. The adopted other parameters are $M = 10^3 M_{\odot}$ and $c_s(\infty) = 10 \text{kms}^{-1}$.

Bondi accretion rates for $\rho(\infty) = 10^{-24} \text{g cm}^{-3}$ (the lower dotted line) and $10^{-22} \text{g cm}^{-3}$ (the upper dotted line). We remark that $\rho(\infty) = 10^{-24} \text{g cm}^{-3}$ is the typical gas density of halos formed at $z \sim 10 - 30$ in standard Λ CDM cosmology. Here, we also assume the sound velocity of $c_s(\infty) = 10 \text{kms}^{-1}$, which corresponds to the halo virial temperature, 10^4K . As shown in this figure, the S-shaped curve shifts toward upper right as the radius increases. It is obvious that these accretion disks would exhibit a limit-cycle behaviour in the regions of $10^3 r_S - 10^4 r_S$, since the Bondi accretion rate corresponds to the middle unstable branches at such regions.

We also investigate the possibility to detect the POP III disks. For this purpose, we try to obtain the disk SEDs in the burst state. Since the disks are very optically thick in this state (see figure 2), we calculate the SEDs by the superposition of the blackbody spectra with various temperatures at the disk surface. Here, we consider the limit-cycle oscillation induced by disk instability at $r \sim 10^4 r_S$. We set the mass-accretion rate to be $2.1 \times 10^{-7} M_{\odot} \text{yr}^{-1}$ for $r > 10^4 r_S$, which is a feasible rate if we assume Bondi accretion from a small dark halo. The mass-accretion rates within $10^4 r_S$ are assumed to be $\dot{M} = 4.5 \times 10^{-4} M_{\odot} \text{yr}^{-1}$.

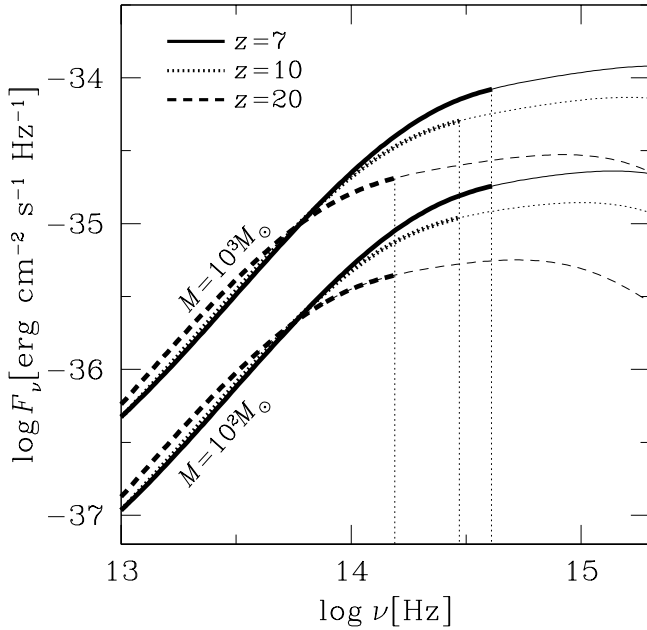


Fig. 4. SEDs of POP III black hole accretion disks with $M = 10^3 M_\odot$ (the three upper lines) and $M = 10^2 M_\odot$ (the three lower lines). Each line type corresponds to $z = 7$ (the solid line), 10 (the dotted lines), and 20 (the dashed lines). The SED break denoted by thin dotted lines at $10^{14} \text{ Hz} \lesssim \nu \lesssim 10^{15} \text{ Hz}$ represents the edge of a Gunn-Peterson trough.

We can estimate the temperature profile of the disk surface using above mass-accretion rates and equation (7), except for the innermost regions. This equation gives the temperature profile of $T \propto r^{-3/4}$. The mass-accretion rate exceeds the critical rate within $r = 10^4 r_S$ (see figure 1). Therefore, photon trapping becomes nonnegligible in the innermost regions of the disk, $r \lesssim (\dot{M} c^2 / L_E) r_S$. In this region, the temperature profile should be modified as $T \propto r^{-1/2}$. Such a profile has been reported by a self-similar solution of the slim disk model (Wang & Zhou 1999; Watarai & Fukue 1999). Watarai et al. (2000) has also shown a similar profile by solving the global solution.

Figure 4 represents the SEDs of face-on POP III disks at three redshifts: $z = 7, 10$ and 20 . The adopted cosmological parameters are $\Omega_M = 0.3$, $\Omega_V = 0.7$, and $h_{0.7} = 1$. We also add a break due to the Gunn-Peterson effect for each SED at $10^{14} \text{ Hz} \lesssim \nu \lesssim 10^{15} \text{ Hz}$. The resulting SED shifts toward lower left as the redshift increases.

In this figure, we also plot the SEDs of POP III disks around black holes with $M = 10^2 M_\odot$. We find that the equilibrium curve with $M = 10^2 M_\odot$ at $r = 5 \times 10^4 r_S$ roughly overlaps with the curve for $M = 10^3 M_\odot$ at $r = 10^4 r_S$. Thus, we consider the limit-cycle oscillation occurs at $r \sim 5 \times 10^4 r_S$. The mass-accretion rates at $r \leq 5 \times 10^4 r_S$ and at $r > 5 \times 10^4 r_S$ are set to be $\dot{M} = 4.5 \times 10^{-4} M_\odot \text{ yr}^{-1}$ and $\dot{M} = 10^{-7} M_\odot \text{ yr}^{-1}$, respectively. We find that the flux

densities in the case of $M = 10^2 M_\odot$ are about 20–30% of those in the case of $M = 10^3 M_\odot$ at $10^{13} \text{ Hz} \lesssim \nu \lesssim 10^{15} \text{ Hz}$.

Those flux densities are quite low for available facilities at present; however, 10 hr integration by OWL telescope manages to reach the flux for $10^3 M_\odot$ around $1 \mu\text{m}$, if they could achieve the same limiting flux at $1 \mu\text{m}$ as V-band ².

4.2. Number of Sources

Here, we evaluate the expected number density of POP III BHs. The number density of POP III BHs could be evaluated by the star-formation rate of POP III stars. Theoretical studies (Sokasian et al. 2004) predict that the comoving star-formation density is roughly $\sim 10^{-3} M_\odot \text{ yr}^{-1} \text{ Mpc}^{-3}$ at $z \gtrsim 20$, although there are still large uncertainties due to various feedback effects (e.g, Susa & Umemura 2006). If we assume all of the POP III stars turned out to be POP III BHs, the number density of POP III BHs is roughly evaluated as follows:

$$n_{\text{P3BH}} = 1.0 \times 10^2 \left(\frac{\text{SFR}}{10^{-3} M_\odot \text{ yr}^{-1} \text{ Mpc}^{-3}} \right) \times \left(\frac{t}{10^8 \text{ yr}} \right) \left(\frac{M}{10^3 M_\odot} \right)^{-1} h_{0.7}^3 \text{ Mpc}^{-3}. \quad (18)$$

Here, t denotes the duration of POP III star formation.

On the other hand, the comoving volume, which corresponds to the observed field of view with $\theta \times \theta$ at $z \sim z + \Delta z$, is

$$V = 1.6 \times 10^4 \left(\frac{\theta}{10'} \right)^2 \left(\frac{\Delta z}{0.1} \right) \times \left[\frac{\phi(z)}{1} \right] \left(\frac{1+z}{11} \right)^{-1} h_{0.7}^3 \text{ Mpc}^3. \quad (19)$$

Here, $\phi(z)$ is a function that equals to almost unity for $z \gtrsim 10$. Finally, we obtain the observed number of sources by multiplying n_{P3BH} , V and the efficiency ϵ (see last paragraph in §3):

$$N_{\text{obs}} = 8.0 \times 10^3 \left(\frac{\theta}{10'} \right)^2 \left(\frac{\Delta z}{0.1} \right) \left(\frac{\epsilon}{5 \times 10^{-3}} \right) \times \left[\frac{\phi(z)}{1} \right] \left(\frac{1+z}{11} \right)^{-1}. \quad (20)$$

Although these are optimistic assessments, it seems possible to find $10^3 M_\odot$ BHs at $z = 10$ if we have telescopes that cover a $10' \times 10'$ field of view with a sufficient limiting magnitude.

As supplementary evidence, we also evaluate the number density of POP III BHs based on the local SMBH density. Yu and Tremaine (2002) assessed the density of massive black holes in the present universe using a simple correlation between the black hole mass and the velocity dispersion of the bulge stars (Gebhardt et al. 2000; Ferrarese & Merritt 2000). If we consider most of the POP III BHs are taken in by massive black holes through merging,

² According to the project URL (http://www.eso.org/projects/owl/index_2.html), OWL will have limiting magnitude of $V \sim 38$.

present-day massive black hole density gives the upper limit of the POP III BH density. In fact, POP III BHs are formed at high-density peaks of a random Gaussian density fluctuation of the universe, which tend to be located within density fluctuations with larger scales, such as galactic scales. Such intermediate-mass black holes in a galaxy settle onto the galactic centre, since they lose their orbital angular momentum through dynamical friction and three-body interaction processes (Ebisuzaki et al. 2001).

According to Yu and Tremaine (2002), the local massive black hole density is given by

$$\rho_{\text{MBH}} = 2.9 \times 10^5 h_{0.7}^2 M_{\odot} \text{Mpc}^{-3}. \quad (21)$$

Thus, the upper limit of the comoving POP III BHs number density at high redshift is

$$n_{\text{P3BH}} = 2.9 \times 10^2 \left(\frac{M}{10^3 M_{\odot}} \right)^{-1} h_{0.7}^2 \text{Mpc}^{-3}. \quad (22)$$

It is suggestive that this predicted number density is only a few-times larger than the value given in equation (18).

5. Conclusions

By solving the vertical structure of the optically-thick accretion disks, including the convective energy transport, and by employing the one-zone model for optically thin isothermal disks, we investigate the stability of the disks in primordial environments.

POP III disks ($Z \lesssim 10^{-4} Z_{\odot}$) are thermally and secularly unstable, and exhibit limit-cycle oscillations, like the POP I disks ($Z \sim Z_{\odot}$). The outbursts of POP III disks are stronger than those of POP I disks. The maximal luminosity in the burst state is expected to be an order of magnitude larger in POP III disks than in POP I disks.

The expected flux densities of POP III disks surrounding black holes of $M = 10^3 M_{\odot}$ are $\sim 10^{-34} \text{erg s}^{-1} \text{cm}^{-2} \text{Hz}^{-1}$ around $1 \mu\text{m}$ in the case of $z \sim 10$, whereas the expected number of sources is $O(10^3)$ per $10' \times 10'$ field of view. Those disks are within reach of future facilities, such as OWL.

Numerical calculations were carried out at Rikkyo University. This work was supported in part by a special postdoctoral researchers program in RIKEN (KO), and by Ministry of Education, Culture, Sports, Science, and Technology (MEXT) Young Scientists (B) 17740111(KO) and 17740110 (HS).

References

Abel T., Bryan G. L., Norman M. L., 2000, ApJ, 540, 39
 Balbus S. A., 2003, ARA&A, 41, 555
 Cannizzo J. K., Wheeler J. C., 1984, ApJS, 55, 367
 Ebisuzaki T., et al., 2001, ApJ, 562, L19
 Ferrarese L., Merritt D., 2000, ApJ, 539, L9
 Gebhardt K., et al., 2000, ApJ, 539, L13
 Bromm V., Coppi P. S., Larson R. B., 2002, ApJ, 564, 23

Ferguson J. W., Alexander D. R., Allard F., Barman T., Bodnarik J. G., Hauschildt P. H., Heffner-Wong A., Tamanai A., 2005, ApJ, 623, 585
 Hawley J. F., Balbus S. A., Stone J. M., 2001, ApJ, 554, L49
 Heger, A. & Woosly, S.E. 2002, ApJ, 567, 532
 Hōshi, R. 1979, Progress of Theoretical Physics, 61, 1307
 Huang M., Wheeler J. C., 1989, ApJ, 343, 229
 Kato, S., Fukue, J., & Mineshige, S. 1998, Black-Hole Accretion Disks (Kyoto: Kyoto Univ. Press)
 Kitayama, T., Yoshida, N., Susa, H. & Umemura, M., 2004, ApJ, 613, 631
 Lin, D. N. C., & Shields, G. A. 1986, ApJ, 305, 28
 Machida M., Matsumoto R., Mineshige S., 2001, PASJ, 53, L1
 Mayer M., Duschl W. J., 2005, MNRAS, 356, 1
 Meyer, F., & Meyer-Hofmeister, E. 1981, A&A, 104, L10
 Meyer F., Meyer-Hofmeister E., 1984, A&A, 132, 143
 Mii H., Totani T., 2005, ApJ, 628, 873
 Mineshige, S., & Shields, G. A. 1990, ApJ, 351, 47
 Mineshige S., Osaki Y., 1983, PASJ, 35, 377
 Mineshige S., Wheeler J. C., 1989, ApJ, 343, 241
 Omukai K., Nishi R., 1998, ApJ, 508, 141
 Ohsuga, K. 2006, ApJ, 640, 923
 Ohsuga, K. 2007, ApJ, 659, 205
 Ohsuga K., Mineshige S., Mori M., Umemura M., 2002, ApJ, 574, 315
 Ohsuga K., Mori M., Nakamoto T., Mineshige S., 2005, ApJ, 628, 368
 Paczyński, B. 1969, Acta Astronomica, 19, 1
 Pringle J. E., 1976, MNRAS, 177, 65
 Rees M. J., 1984, ARA&A, 22, 471
 Ricotti M., Ostriker J. P., 2004, MNRAS, 352, 547
 Shakura N. I., Sunyaev R. A., 1976, MNRAS, 175, 613
 Shibazaki N., Hōshi R., 1975, PThPh, 54, 706
 Sokasian A., Yoshida N., Abel T., Hernquist L., Springel V., 2004, MNRAS, 350, 47
 Smak, J. 1982, Acta Astronomica, 32, 213
 Susa H., Umemura M., 2006, ApJ, 645, L93
 Tuchman, Y., Mineshige, S., & Wheeler, J. C. 1990, ApJ, 359, 164
 Wada K., Venkatesan A., 2003, ApJ, 591, 38
 Wang, J.-M., & Zhou, Y.-Y. 1999, ApJ, 516, 420
 Watarai K.-y., Fukue J., 1999, PASJ, 51, 725
 Watarai, K.-y., Fukue, J., Takeuchi, M., & Mineshige, S. 2000, PASJ, 52, 133
 Watarai, K.-Y., Ohsuga, K., Takahashi, R., & Fukue, J. 2005, PASJ, 57, 513
 Yu Q., Tremaine S., 2002, MNRAS, 335, 965